Petroelasticity: Assessing Rock Properties under Stress through (Often) Non-Destructive Tests

Guilherme Vasquez, Marcio Morschbacher, Julio Justen and Douglas Lacerda, Petrobras.

Abstract

The record of the transition of rock properties with stress changes is extremely important for petroleum exploration and reservoir development. Unfortunately, even the behavior of elementary rock attributes, such as porosity and seismic velocities are not completely understood, at least for some boundary conditions. For instance, there are disagreements regarding the seismic velocity behavior under anisotropic stress conditions. Some authors claim that the average effective stress is the governing parameter, while others suggest that the average method is more complex than the simple arithmetic mean. Actually, the fundamental concept of effective stress is sometimes a matter of discussion. In this paper, we present and discuss experimental results on the evolution of porosity and seismic velocities under several different stress paths. Our goal is to test some plausible boundary conditions and their influences on velocity and porosity, aiming to get an insight of the possible errors involved in adopting usual approximations and simplifications.

Introduction

There is no doubt about the importance of laboratory testing for obtaining rock properties, such as permeability, porosity and wave velocity for hydrocarbon exploration and production. Nevertheless, in general, most of the laboratory tests are conducted under hydrostatic stress states due to productivity issues or even due to our ignorance about the real in situ stress state. In this work we are particularly interested on the porosity and velocity evolution with different stress states and stress paths.

In spite of important existing results on the literature, both on theoretical and on experimental sides, it seems that there is still some disagreement on the translation of usual vintage laboratory data to true *in situ* values regarding more complex situations. For example, both Shafer *et al*. (2008) and Vasquez *et al*. (2010) suggest that the mean effective stress is the main boundary condition governing the seismic velocities. If the rock was subjected to the effective stresses σ'_1, σ'_2 and σ'_3, it would have the same velocities in a hydrostatic condition where the effective stress is $(\sigma'_1+\sigma'_2+\sigma'_3)/3$, or $(\sigma'_V+2\sigma'_H)/3$ for equal horizontal stresses. On the other hand, Sayers and Ghose (2011) claim that the stress averaging method for seismic velocities may be modified, they had shown that the shear modulus depends on the combination $(2\sigma'_V+3\sigma'_H)$. In other words, the simple arithmetic mean of effective stresses should not be applied.

Furthermore, the pore compressibility, C_ϕ, so important for the initial production forecast, is usually measured under hydrostatic confining stress. Laboratory results are "translated" to uniaxial pore compressibility by a simple law, multiplying the lab result by $\{[(1+\nu)/(1-\nu)]/3\}$, where ν is the Poisson's ratio, usually assumed as 0.3 for this transformation.

Based on these examples, as well as on other daily used shortcomings, we strongly believe that more and more experimental investigations are welcome and necessary. Moreover, although we refer to our problem as "petroelasticity", it has viscous and plastic contributions that sometimes are far from being negligible.

This paper presents contributions on the understanding of porosity and velocity evolution with stresses for a variety of boundary conditions.

Experimental Method

Compressional and shear-wave propagation velocities, V_P and V_S, and also the pore volume variation, were measured with an adapted velocity core holder that allows imposing stress conditions with axial symmetry. The experimental apparatus is schematically shown in Figure 1.

Vertical (axial) and horizontal stresses were imposed separately with two pressure controllers for geotechnical applications. Pore pressure was applied with the aid of a syringe pump that had the ability to measure volumes within hundredths of milliliters. Sample length was monitored within thousandth of millimeters. This system was also equipped with damped transducers built in a sandwich configuration, each one with a P-wave and two mutually orthogonal S-wave piezoelectric elements, and velocities were measured by the pulse transmission method. It is worth noticing that, although the stresses and pore pressure may be carefully controlled, this is not a servo-controlled rock mechanics cell.

Several different combinations of stresses and stress paths were tested to track the porosity and velocity variation of rock samples. Both real reservoir and outcrop rocks were used, since our interest was not focused on a particular geological formation, but on the general effect of stress conditions. Due to available space issues, only few representative cases will be presented in this paper.

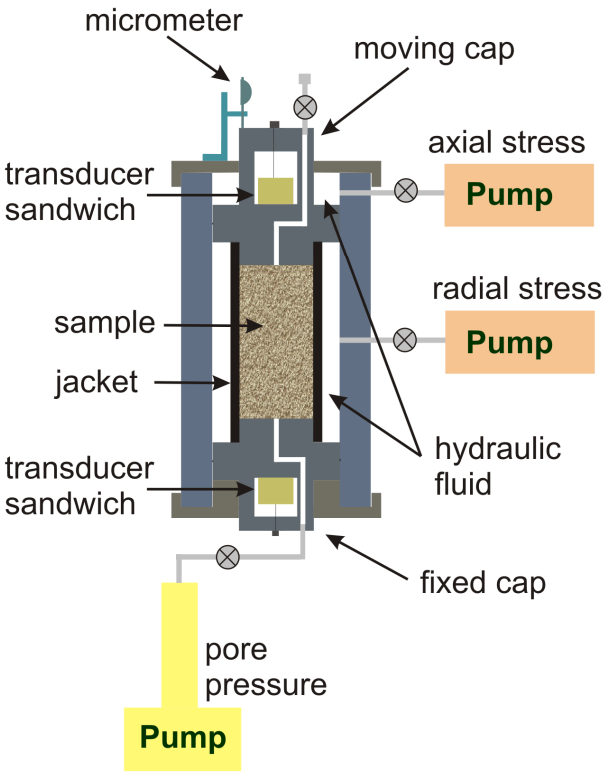

Figure 1- Schematic configuration of the experimental setup.

Results

Several series of experiments were conducted under different conditions, the protocol depending on the particular interest. Cases of anisotropic stress compression and cyclic hydrostatic compression with porosity monitoring will be shown here.

Velocity and Anisotropic Stress Compression

The anisotropic stress compression tests involved the compression of rock samples for different horizontal to vertical stress ratios, σ_H/σ_V while the P and S-wave velocities, porosity and sample length were monitored.

As the first example of anisotropic compression, Figures 2 and 3 show respectively the compressional and shear waveforms recorded for a Leopard Sandstone sample, with 15.73% porosity. This test aimed to access the velocity behavior for anisotropic stress states, and it consisted in compressing the sample up to 60 MPa vertical stress with the stress ratios, σ_H/σ_V equal to 100, 80, 60, 40 and 20 %. The pore pressure was maintained fixed at 1.38 MPa, while the vertical stress was increased from 2.5 to 60 MPa, the lateral stress were imposed accordingly. For σ_H/σ_V=0.4 the initial vertical stress was 5 to avoid fluid leaking from the sample jacket. Note that the ratio σ_H/σ_V=0.2 contains a smaller number of wave trains, because the sample had failed during the test. The failure process is accompanied by a strong decrease in the amplitude and "quality" of the shear waveforms. Actually, even for σ_H/σ_V =0.4 the shear wave first arrival is very difficult to identify, especially for the lowest stress values.

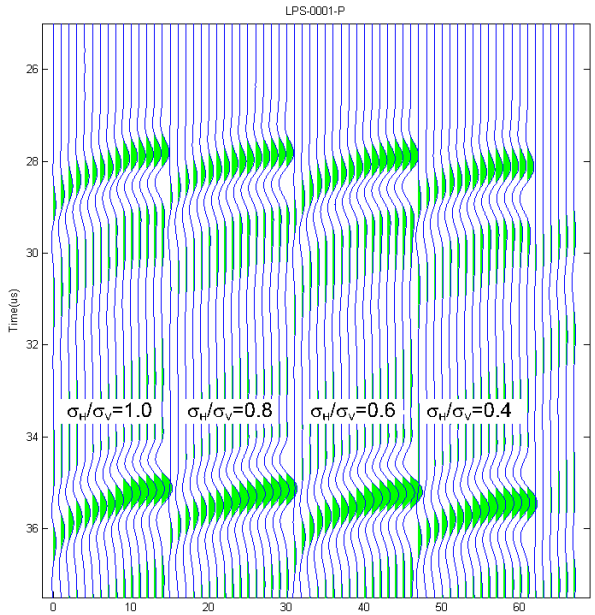

Figure 2 – P-wave pulses for the Leopard Sandstone sample LPS001. The stress ratio σ_H/σ_V is indicated in each waveform sequence, the one at right side corresponds to σ_H/σ_V=0.2, not shown due to space.

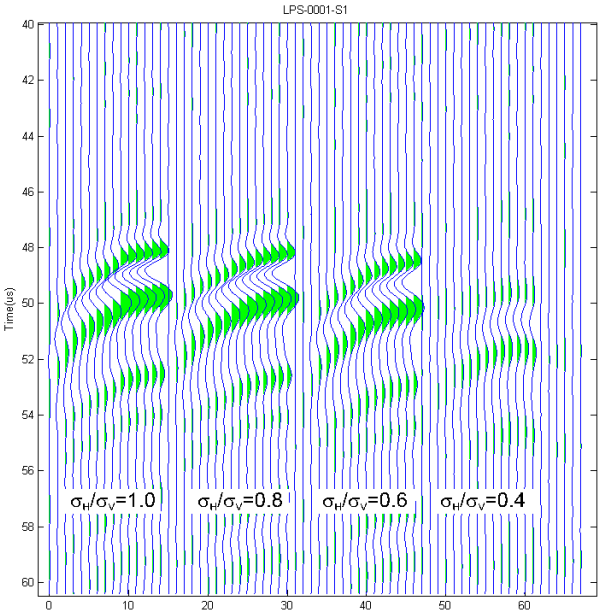

Figure 3 – S-wave pulses for the Leopard Sandstone sample LPS001. The stress ratio σ_H/σ_V is indicated in each waveform sequence, the one at right side corresponds to σ_H/σ_V=0.2, not shown due to space.

The behavior of P-wave velocity and V_P/V_S ratio with vertical stress are illustrated on Figures 4 and 5, respectively. It can be noticed that, for larger lateral compressions, the velocity gradient with vertical stress is larger, although for 1 and 0.8 stress ratios the behavior is quite similar and there is a switch for smaller stresses. The V_P/V_S ratio decreases with increasing axial stress, as can be observed in Figure 5, but its gradient is not so sensitive to the σ_H/σ_V ratio. It is probable that there is a problem on the V_P/V_S ratio for low stress (less than 10 MPa) due to uncertainty in S-wave determination, introducing relatively high V_P/V_S values.

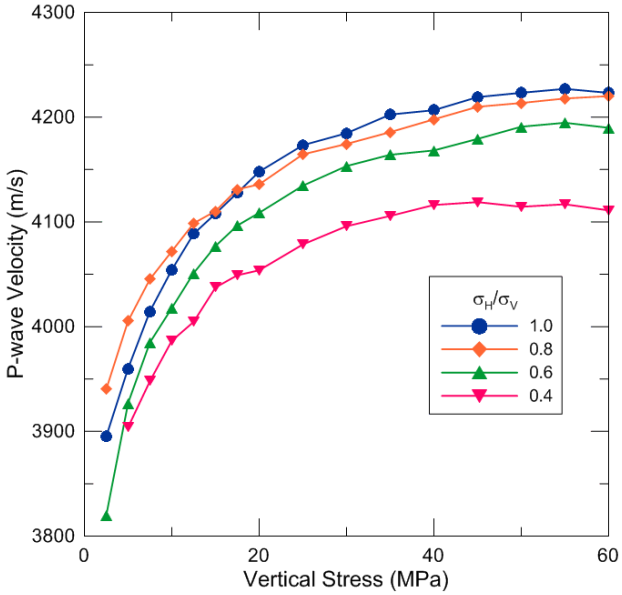

Figure 4 – P-wave velocity as a function of increasing vertical stress for different horizontal to vertical stress ratios on the Leopard Sandstone LPS001.

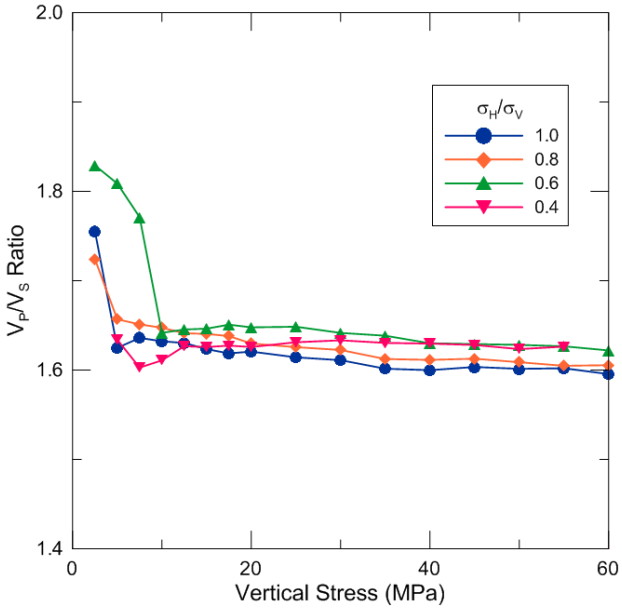

Figure 5 – V_P/V_S ratio as a function of vertical stress for the Leopard Sandstone sample LPS001.

The P-wave velocity for different vertical stresses is illustrated on Figure 6, as a function of the horizontal to vertical stress ratio σ_H/σ_V. This graph highlights the importance of the stress ratio on the velocity behavior with stress.

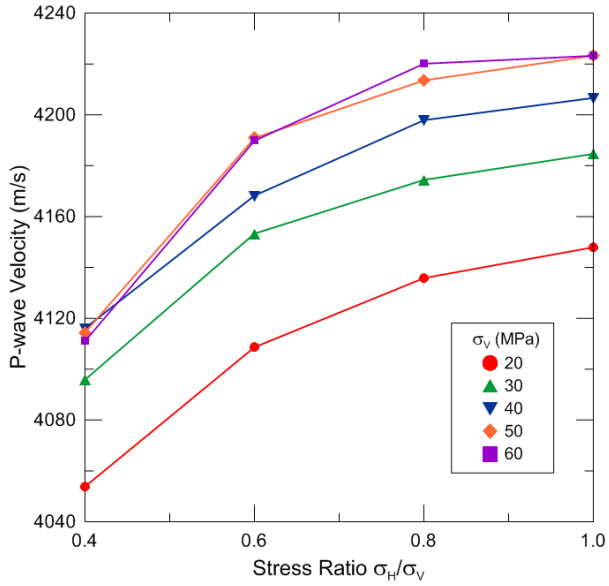

Figure 6 – Velocity as a function of the horizontal to vertical stress ratio for different vertical stress values, for the Leopard Sandstone sample LPS001.

The P-wave velocity behavior with mean effective stress is plotted in Figure 7, in order to check the role of average stress on velocities. There is an impressing overlapping among the curves for different stress ratios, except for the ratio of 0.4, maybe due to the beginning of rock damage process, as suggested by the lower S-wave amplitudes and velocities (cf. Fig. 3). If we plot the velocity curves as a function of $(3\sigma'_H+2\sigma'_V)$ the graph appearance is similar.

Although the velocity gradient with vertical stress depends on the horizontal to vertical stress ratio σ_H/σ_V, there may not be a general universal behavior. Several horizontal to vertical stress ratios were tested for a variety of sandstones, indicating the rock composition and texture may also have an impact on the velocity gradient changes

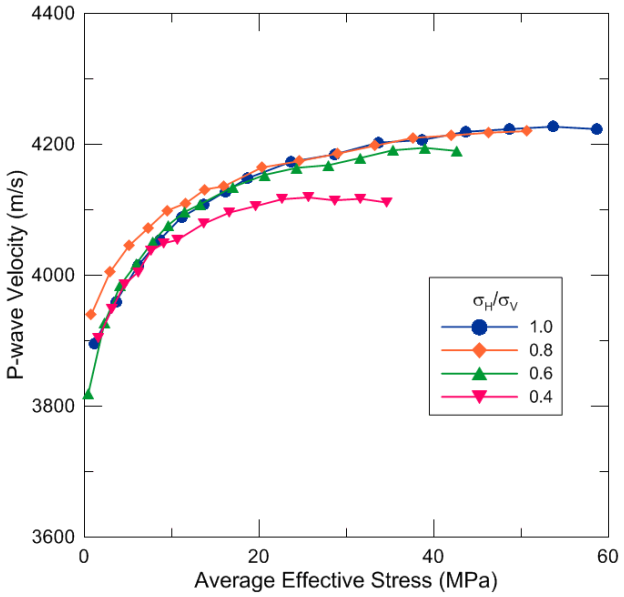

Figure 7 – P-wave velocity as a function of average effective stress, $[(\sigma_V+2\sigma_H)-3P_p]/3$.

Similar laboratory tests involving vertical compression with different σ_H/σ_V ratios were carried out for a Sister Gray Berea Sandstone, with 19.47 % porosity. In this case, the velocity gradients with axial stress observed for σ_H/σ_V ratios of 100, 80 and 60 % were very similar, some differences being observed for 40 and 20 %, as can be noted from the velocity curves as a function of axial stress, shown in Figure 8. It is believed that the sample is damaged for all the σ_H/σ_V=0.2 stress cycle, since the velocity for lower stresses is smaller. The low velocity value for 50 MPa axial stress corresponds to a dramatic sample compaction due to the failure process.

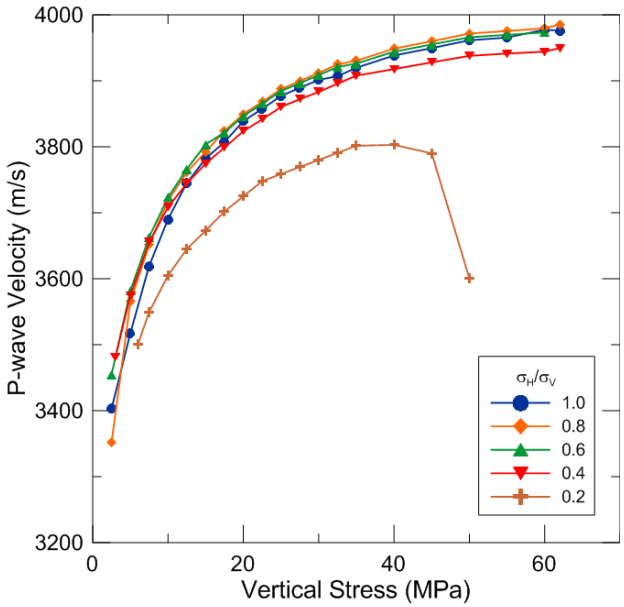

Figure 8 – P-wave velocity evolution with increasing axial stress for several horizontal to vertical stress ratios, σ_H/σ_V, for the Berea Sandstone sample SGS003.

A third example on velocity gradient, associated to the anisotropic compression of a Bandera Brown Sandstone with 16.63 % porosity, is illustrated on Figures 9 and 10. The first figure shows the velocity with increasing axial stress for the stress ratios σ_H/σ_V changing from 1.0 down to 0.4 with 0.1 decrements. Axial compression was made from 2.5 up to 62 MPa, with a constant pore pressure of 1 MPa. The difference in velocity gradient with stress is not as clear as on the previous examples and the curve for σ_H/σ_V=0.4 indicates lower velocities, probably related to the beginning of sample damage. The evolution of porosity with axial stress, however, shows a systematic change, as can be seen in Figure 9, with curves for smaller σ_H/σ_V ratios apparently more concave and exhibiting lower porosities for the same axial stress. Note that the porosity curve for σ_H/σ_V=0.4 does not follow the general behavior, maybe due to the sample damage, indicated by lower porosities, caused by the compaction, followed by sample rupture.

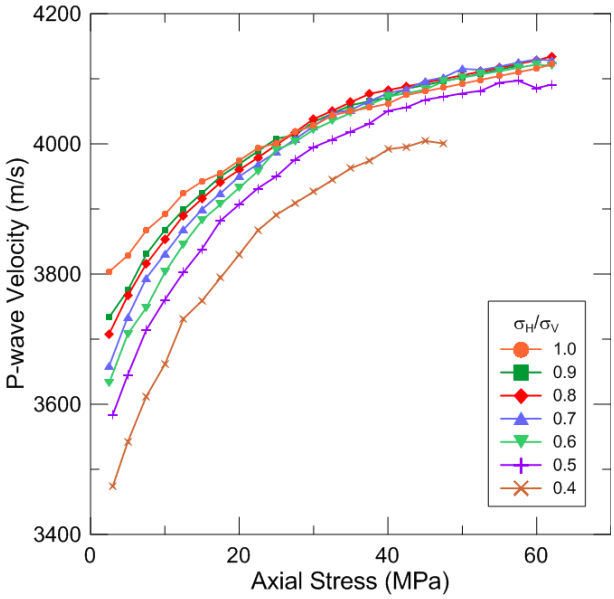

Figure 9 – P-wave velocity evolution with increasing axial stress for several horizontal to vertical stress ratios, σ_H/σ_V for the Bandera Sandstone sample BBS004.

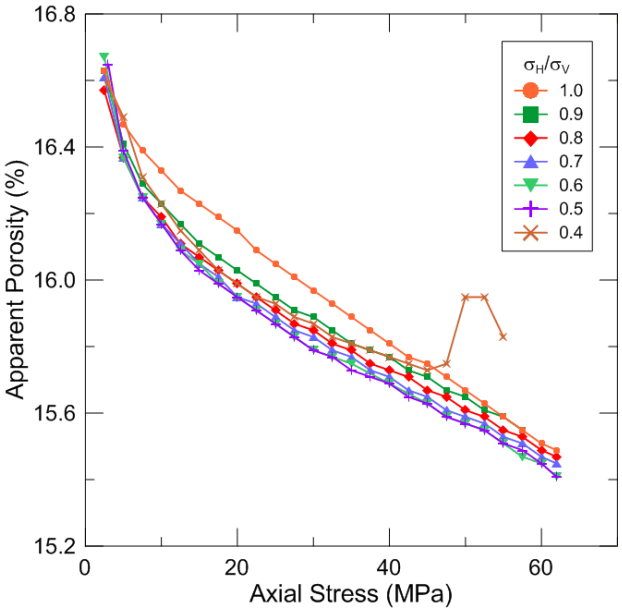

Figure 10 - Porosity evolution with increasing axial stress for several horizontal to vertical stress ratios, σ_H/σ_V for the Bandera Sandstone sample BBS004.

Cyclic Hydrostatic Compression Tests

Another interesting laboratory protocol consisted of varying the pore pressure maintaining the confining stress at a constant value. This is the same procedure used in conventional pore compressibility tests. Alternatively, the confining stress can be varied at a fixed pore pressure state. This corresponds to a pore compressibility test to obtain the "formation compaction" coefficient. The samples were eventually submitted to several cycles or stages of stress paths, in order to test hysteresis issues.

One example of such test on a Berea Sandstone sample, with 19.17% porosity, is illustrated on Figure 11 for the P-wave velocity, and on Figure 12 for the porosity. Notice that, for this sample, the first stage begun with the sample under a 62 MPa confining stress and 35 MPa pore pressure. Then, the pore pressure was increased up to 61.5 MPa. On the second stage confining stress was fixed on 62 MPa and the pore pressure dropped from 61.5 to 2.5 MPa. Finally, on the third stage the pore pressure were increased from 2.5 up to 61.5 MPa. Although there is some velocity difference between the three different stages, it might be considered relatively small, since it's about 1% of the velocity itself, and the hysteresis can be neglected. The porosity for the first and second stages follows the same trend, assuming lower values on the last one. We are not sure if this difference may be attributed to some experimental factor or not.

Hydrostatic compression tests were conducted also with real reservoir sand samples. Figure 13 illustrates the P-wave velocity and Poisson's ratio behavior with differential stress for a clean, unconsolidated sandstone sample from an offshore Brazilian oil field. In this case the confining stress was fixed at 42 MPa, and pore pressure varied from 41.9 to 0.1 MPa, and then increased again up to 41.9 MPa. Surprisingly the hysteresis may be negligible, and the difference on Poisson's ratio for lower effective stress is actually due to poor quality of S-wave velocity picking. We are not confident on the porosity evolution with stress for this sample, although an apparent perfect cycle, as those from Figure 12, were observed, and the result is not shown here.

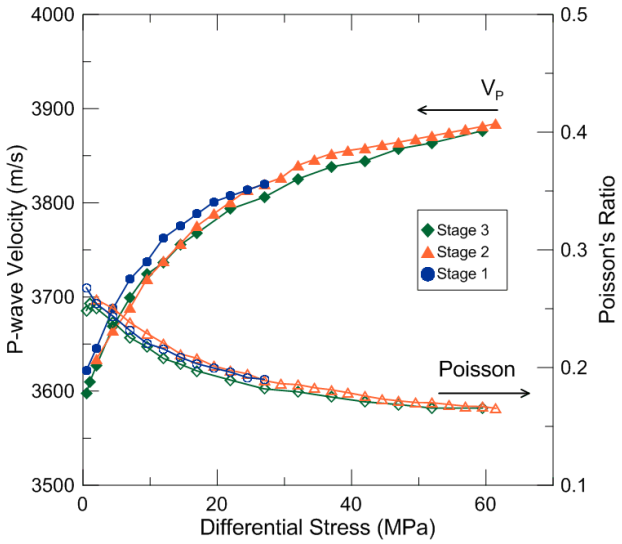

Figure 11 – Evolution of the P-wave velocity (full symbols) and Poisson's ratio (open symbols) of a Berea Sandstone with effective (hydrostatic) stress.

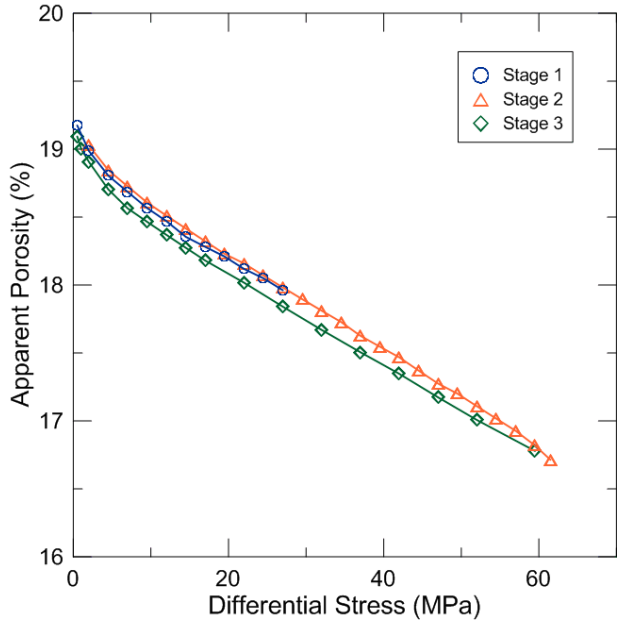

Figure 12 – Porosity evolution during loading and unloading cycles on a Berea Sandstone sample.

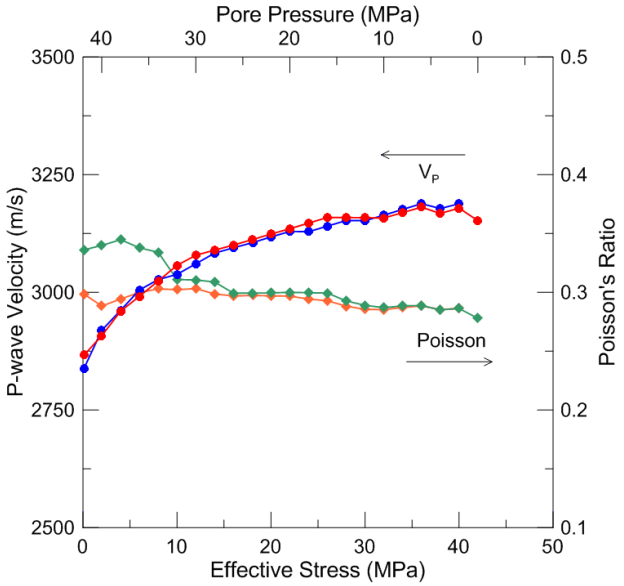

Figure 13 – P-wave velocity (red and blue discs) and Poisson's ratio (Green and Orange Diamonds) for an unconsolidated sand reservoir rock.

Discussion and Future Developments

Examples on velocity and porosity behavior for different stress states and stress paths were presented.

Regarding the velocity evolution under anisotropic stress conditions, differences in the velocity gradient with axial stress were observed. Nevertheless, this difference is not evident for all horizontal to vertical stress ratio for some rocks. It seems that the rock composition and texture plays some role in this dependence. Efforts on a better characterization of the different rocks used in our study are ongoing to confirm and explain this statement. More laboratory tests under similar conditions are being conducted as well. The porosity evolution with anisotropic stress compression also depends on the stress ratios.

During cyclic loading of rock samples minor hysteresis effects were observed for some rocks. On the other hand, it is well known, by our experience, that this is not a ground truth for every rock. In some cases, irreversible changes in rock texture, maybe involving rearrangements of grains and other microscopic stress effects, introduces notable hysteresis on velocity and porosity behavior with stress.

Although the series of laboratory experiments discussed on this paper did not lead us to final conclusions, it reinforces the indisputable need of more lab testing.

Acknowledgments

The authors thank Petrobras for the permission to publish this paper. We strongly thank Angela Vasquez and Carlos Theodoro for the revision and useful suggestions on the manuscript and Andre Romanelli for fruitful discussions on the experimental results.

References

Sayers, C., Ghose, R., 2011, Stress-Induced Anisotropy in Soft Sediments: 1st International Workshop on Rock Physics. August 7 – 12, Colorado School of Mines, Golden, Colorado, USA.

Shafer, J. L., Boitnott, G. N., and Ewy, R. T., 2008, Effective stress laws for petrophysical rock properties: SPWLA 49th Annual Logging Symposium, May 25-28, Edinburgh, Scotland.

Vasquez, G.F., Justen, J., Santos, M.S., Morschbacher, M., Sansonowski, R., Carvalho, M.J., Vargas Jr., E. and Formento, J-L. 2010, Stress history of producing reservoirs and 4D seismic studies: Some often-forgotten aspects: The Leading Edge, 29 (7), pp. 814-818.